Available online at www.sciencedirect.com
SCIENCE DIRECT
Catalysis Today 113 (2006) 48–57
CATALYSIS TODAY
www.elsevier.com/locate/cattod

From conventional in situ to operando studies in Raman spectroscopy

M. Olga Guerrero-Pérez [a,*], Miguel A. Bañares [b]

[a] Departamento de Ingeniería Química, Facultad de Ciencias, Universidad de Málaga, E-29071 Málaga, Spain
[b] Instituto de Catálisis y Petroleoquímica, CSIC, Marie Curie, 2, E-28049 Madrid, Spain

Available online 28 December 2005

Abstract

The determination of the structure–activity relationships at a molecular level requires determining both, structure and activity. Such determination is best made if both are determined in the same experiment. This contribution presents the possibilities of both in situ and operando studies to understand catalysis. Some examples based on the authors' work are presented to illustrate the capabilities of in situ and operando studies.

Keywords: In situ; Operando; TP-Raman; TPR; TPO; Oxidative dehydrogenation; Ammoxidation; Oxidation

1. In situ spectroscopy

Many chemical reactions require a catalytic material; catalysts are a very important group of materials that are required for our society. So, many efforts are focused in the study of these materials, their structures, their catalytic behavior, the reaction mechanisms in which they are involved and the structure–activity/selectivity relationships (SAR). The study of the events that take place in catalysts during reaction would allow understanding how chemical processes operate and, in turn, it will allow for the rational design of better catalytic materials.

Conventional spectroscopy studies fresh, calcined, and used catalysts under conventional conditions: room temperature. Thus, catalysis studies were built on analysis of fresh and used catalysts. The studies of fresh and used catalysts are very informative [1]. However, the actual state of a catalyst during catalytic operation may not be that presented before or after reaction, even if it is under in situ dehydrated conditions [2–5]. The strong relevance of environment on the actual catalyst structure during operation is the driving force to combine in situ studies under actual catalytic operation with simultaneous activity measurement. Such combination of experiments is the concept of Operando Methodology. The term in situ (which means ''on site'') has been used to describe spectroscopic studies involving absorption/desorption processes, catalysts in a controlled environment and temperature, or studies performed under high pressure [6]. In general, in situ is a term used when the conditions of pressure, atmosphere and temperature are controlled during acquisition, or the sample is not exposed to ambient conditions after specific treatments. In situ spectroscopic characterization of catalysts is performed by an arsenal of spectroscopic techniques: infrared (IR), Raman, X-ray absorption (XAS), nuclear magnetic resonance (NMR), electronic spectroscopy in the UV–vis region (UV–vis), electron paramagnetic resonance (EPR), sum frequency generation (SFG), and Mössbauer spectroscopy, among others [1–7].

Many of these techniques are compatible with a design of an in situ cell suitable for genuine catalytic studies by simultaneous determination of kinetic information. Several groups have accomplished it in recent years. Raman spectroscopy is particularly suited for these kinds of studies since it is able to provide fundamental information about the molecular structures of catalysts and about the surface reaction intermediates. In most cases, it uses visible radiation, which makes the design of the in situ cell in glass or quartz particularly convenient. It has been used to examine almost all types of catalytic materials: bulk and supported metals, bulk mixed metal oxides, supported metal oxides, bulk and supported metal sulfides, zeolites and molecular sieves, heteropolyoxo anions and clays [8–30] also in homogenous catalysis [31] and for

* Corresponding author. Tel.: +34 952 13 3448; fax: +34 952 13 2000.
E-mail address: oguerrero@uma.es (M.O. Guerrero-Pérez).

0920-5861/$ – see front matter © 2005 Elsevier B.V. All rights reserved.
doi:10.1016/j.cattod.2005.11.009

enzymes [32]. The combination of Raman molecular structural information and in situ capabilities has resulted in the development of a molecular/level understanding of structure–active/selectivity relationships for catalytic reactions [3–5,9,33–42]. A detailed revision of such Raman works under reaction conditions can be found elsewhere [8,43]. This contribution aims at illustrating the potential of in situ and operando Raman studies through some specific examples in our group.

2. Some examples with in situ Raman spectroscopy

Raman in situ studies can follow the transformations of catalysts upon different treatments, like the chemisorption of molecules (probes or reactants), transformation under different environments (inert, air, reaction, reducing, etc.) [33,35–43]. Such information is very informative on the molecular states of the catalysts under different conditions and reactivities of the different functional groups.

2.1. Thermal treatments

In situ Raman studies under controlled temperature may follow transformations occurring during thermal treatments or preparation of catalysts in air. The thermal decomposition of 1,2-molybdophosphoric acid (HPMo) supported on silica and Zr-loaded silica was monitored with temperature-programmed (TP) Raman spectroscopy [44]. Fig. 1 shows representative in situ TP-Raman spectra of HPMo supported on silica (Fig. 1A) and supported on Zr-loaded silica (Fig. 1B) at different temperatures in dry air stream, molybdenum loading is near 23 wt.% in both samples. $HPMo/SiO_2$ and $HPMo/ZrO_2/SiO_2$ exhibit the Raman bands characteristic of the heteropolyanion with Keggin structure at 50 °C. At 550 °C, the Raman spectra of both samples are quite different. On silica support, the broad band at about 900 cm^{-1} of $HPMo/SiO_2$ spectrum (Fig. 1A) shifts to ca. 863 cm^{-1}, characteristic of β-MoO_3 phase. The sample also exhibits new well-resolved peaks at 993, 861, and 818 cm^{-1} and a small one at 280 cm^{-1}, characteristic of α-MoO_3, evidencing a mixture of α- and β-MoO_3 phases. Intense bands at 993 and 816 cm^{-1} and weaker ones at 657, 333, and 282 cm^{-1}, associated with the bulk α-MoO_3 phase, dominated the spectra at 650 °C. This is expected since α-MoO_3 is stable at higher temperatures. When temperatures increase on the zirconia/silica supported HPMo sample, a new band near 992 cm^{-1} appears (Fig. 1B). This band is sensitive to hydration and is assigned to isolated molybdenum oxide species on zirconia. The Raman spectra of $HPMo/ZrO_2/SiO_2$ sample at 650 °C (Fig. 1B) corresponds to the $Zr(MoO_4)_2$ phase, also detected by XRD on that sample. So, in contrast to silica-supported HPMo, the ZrO_2/SiO_2 support breaks HPMo into surface-dispersed molybdenum oxide species and $Zr(MoO_4)_2$ [44] upon heating but did not form the MoO_3 phase due to a strong Mo–Zr interaction.

In situ TP-Raman studies also provide information on the preparation of a catalyst. Vanadium–phosphorous–oxygen catalysts (VPO) are commercial catalytic system for the selective oxidation of *n*-butane to maleic anhydride. Mesostructured VPO phases were prepared under mild conditions by reacting aqueous solutions containing vanadium ($VOSO_4$) and phosphorus (H_3PO_3 or H_3PO_4) sources in the presence of surfactants, as described elsewhere [45]. Phase transformations in mesostructured VPO phases were studied during thermal treatment in N_2 at 400 °C [46]. The transformation of lamellar-to-hexagonal phase is shown in Fig. 2A. Raman bands corresponding to symmetric P–O–P stretch (790 cm^{-1}), V–O–P stretches (1070 and 1130 cm^{-1}) and P–O stretch (1300 cm^{-1}) [47] are no longer visible above 200 °C. The characteristic C–H and C–C bands of the surfactant were present at 2900 and 1450 cm^{-1}, respectively; these bands are not observed above 150 °C, which is indicative of the progressive decomposition of the surfactant. Two new Raman bands near 1590 and 1350 cm^{-1} became evident as the treatment temperature increased. These bands most likely correspond to the sp^2 carbon in graphite-like materials; due to carbon deposits generated from occluded surfactant molecules. The lack of second-order Raman spectra of the carbonaceous deposits at 2700–3200 cm^{-1} underlines the lack of long-range order of these aggregates. In addition, the relative intensity of these Raman bands at 1590 and 1350 cm^{-1} indicate that the graphite-like deposits domains are roughly below 60 Å, according to Tuinstra and Koenig [48]. These results are

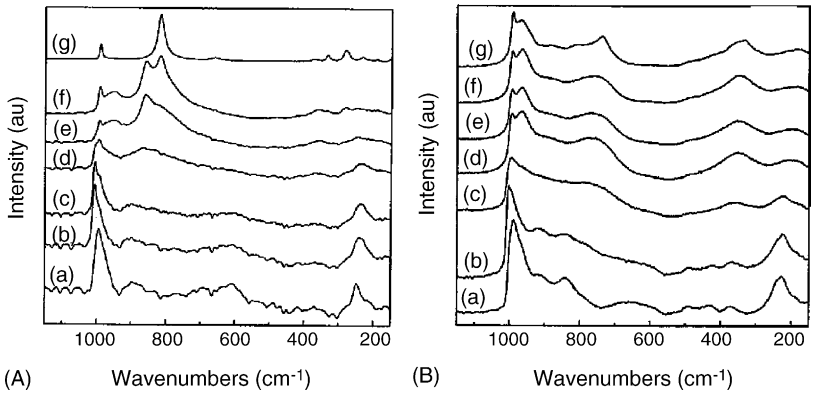

Fig. 1. In situ Raman spectra of $HPMo/SiO_2$ (A) and $HPMo/Zr–SiO_2$ (B) at different temperatures. Part A was read at (a) 323 K, (b) 523 K, (c) 623 K, (d) 723 K, (e) 773 K, (f) 823 K, and (g) 923 K. Part B was read at (a) 323 K, (b) 423 K, (c) 523 K, (d) 623 K, (e) 723 K, (f) 823 K, and (g) 923 K.

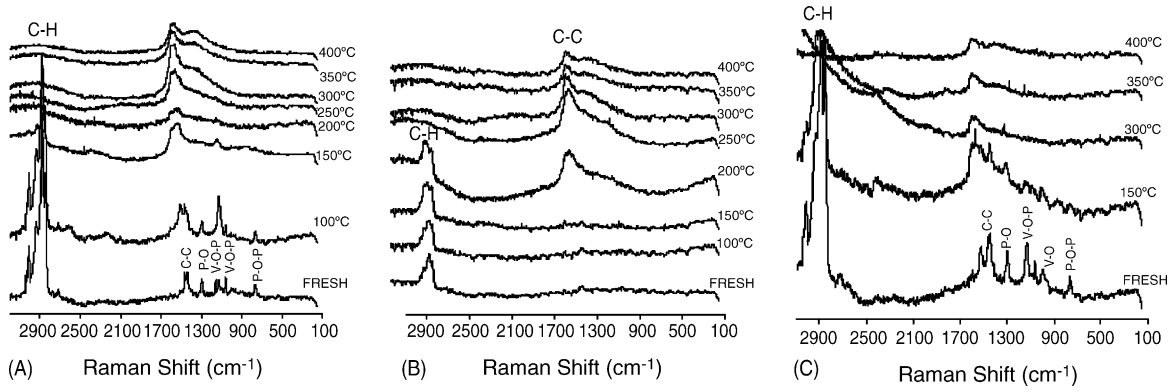

Fig. 2. In situ Raman spectra of mesostructured VPO during the lamellar-to hexagonal (A), hexagonal-to-disordered (B), and cubic-to-amorphous (C) phase transformations in nitrogen atmosphere. Reprinted from Ref. [46], with permission from Elsevier.

consistent with the small size of these carbon deposits, probably constrained by the mesoporous structure. Only the characteristic C–H and C–C vibrations corresponding to the occluded surfactant (2900 and 1450 cm^{-1}) are present in the Raman spectrum of the hexagonal phase (Fig. 2B). The Raman spectrum of the cubic phase shown in Fig. 2C exhibited all the Raman bands previously observed in the Raman spectra of the lamellar phase and one additional band at 1000 cm^{-1} assigned to the V–O mode of the V=O bond, as temperature increases, the structural order was progressively lost, leading to an amorphous material.

2.2. Reduction and oxidation (TPR and TPO)

Temperature-programmed in situ Raman spectroscopy was used to molecularly understand the effect of surface coverage on the reduction/reoxidation profiles of V_2O_5/SiO_2 catalysts [49]. Spectra of a sample with low coverage (30% of monolayer, 0.90 wt.% V_2O_5) and high coverage (near monolayer, 3.36 wt.% V_2O_5) on silica (Degussa Aerosil-200, 174 m^2/g) during TPR and TPO are shown in Fig. 3. The broad Raman bands near 495, 606, 802 and 907 cm^{-1} correspond to the silica support. At low coverage, the Raman band at 1037 cm^{-1} corresponds to the V=O mode of isolated V oxide species and disappears as the reduction of vanadia progresses; these species are fully restored during TPO treatment (Fig. 3A and B). The presence of only isolated vanadium oxide species below monolayer on silica has been confirmed by ^{51}V-spin echo MAS NMR and Raman spectroscopy [50]. The spectra of a sample with high coverage (80% of monolayer coverage) during the TPR and TPO cycles evidence irreversible changes. For this sample, new Raman bands of crystalline vanadia became evident and then disappear with temperature during the TPR (Fig. 3C). At higher temperature, the V=O mode of the remaining isolated vanadia species also disappear. The TPO Raman spectra underlines the irreversible formation of crystalline V_2O_5. These must originate from the rearrangement of surface isolated vanadium oxide species (Fig. 3D). At high vanadia coverage the redox cycles do not appear to follow a reversible transformation since crystals of V_2O_5 cannot be redispersed upon calcination [49]. At low coverages, the transformation to crystals does not happen and the surface isolated vanadium oxide species are restored upon reoxidation (TPO). So, in situ Raman spectroscopy reveals a rearrangement of surface vanadia species under reduction at loading values close to its dispersion limit. Surface vanadium oxide species have some mobility, but the chances to aggregate depend on the probability to interact with other surface vanadium sites. Such probability increases with surface coverage. The interaction between surface vanadium sites provides the possibility to share oxygen-sites on reduction, leading to V–O–V bond formation between surface isolated vanadium oxide species. This would be the driving force to aggregate surface vanadium oxide species on reduction, which accounts for the loss of dispersion of supported vanadia catalysts under repeated cycles [51]. Therefore, vanadia coverage would have a clear effect on reduction profiles. As coverage increases, the chances for major rearrangement of surface vanadium oxide species intro crystalline V_2O_5 increases. This would have an effect on the reduction process that should show in the TPR profiles. Actually, quantitative TPR profiles of supported vanadia catalysts are described by a linear combination of two phenomena: random nucleation and bidimensional nuclei growth; the former becomes increasingly dominant with vanadia coverage [52]. This is consistent with the structural changes observed during TPR/TPO Raman studies at different coverages. Similar rearrangements of surface vanadium oxide species near monolayer coverage have also been observed for alumina-supported vanadium oxide species [53]. Reduced vanadium oxide species show no intense Raman bands, so it is not possible to assess the actual state of the reduced phase. However, the molecular structures after reoxidation indicate if vanadium species rearrange on reduction. Thus, in situ TP-Raman studies during reduction/reoxidation provide information to molecularly understand the transformation of oxides during these treatments.

In situ TP-Raman spectroscopy was used to investigate the synergistic effect of Pt incorporated to CoZSM5 catalysts for the reduction of NO with methane [54]. These catalysts were prepared by ionic exchange starting from NaZSM5. Monometallic cobalt-exchanged NaZSM5 solids were prepared using cobalt acetate solution, with 10 g/1.5 l (zeolite/solution) ratio

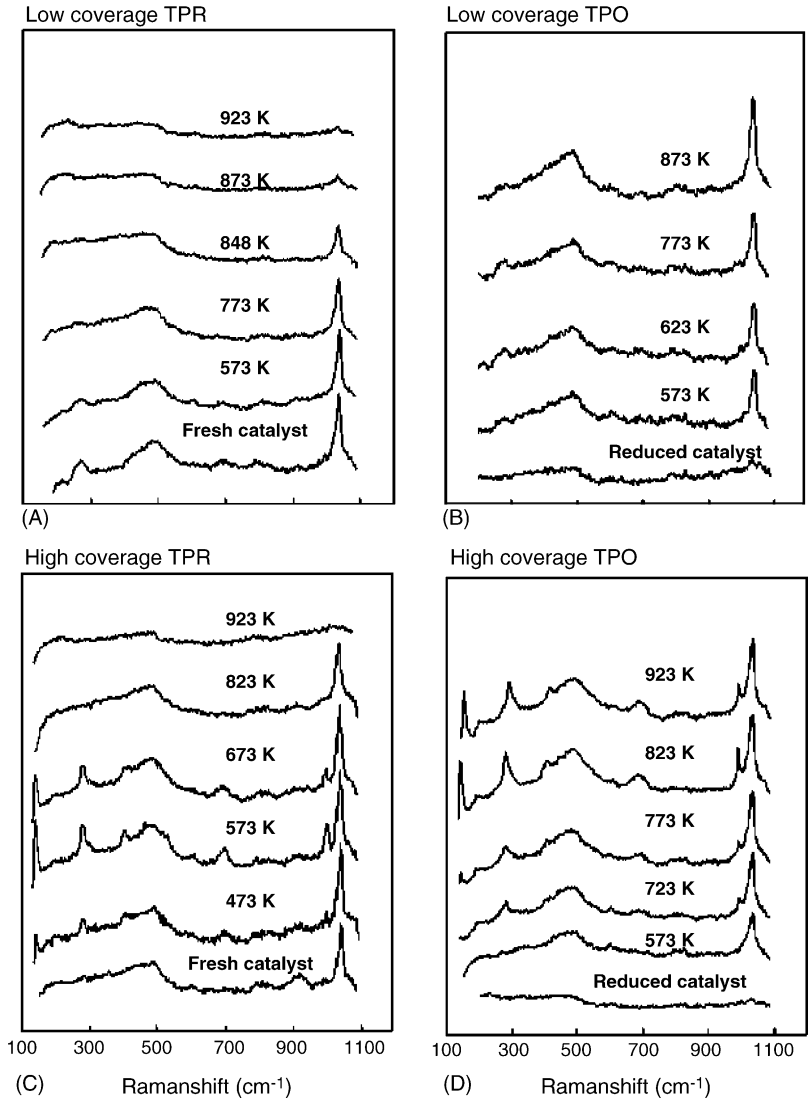

Fig. 3. Selected in situ Raman spectra of silica-supported vanadia catalyst with low coverage during the TPR Raman of a fresh dehydrated sample (after calcination) (A) and during the TPO Raman of the reduced simple (B); catalyst with high coverage during the TPR Raman of a fresh sample (C) and during the TPO Raman of the reduced sample (D).

[54]. Raman spectra of fresh and used CoZSM5 are shown in Fig. 4A (b and c). The Raman modes of the zeolite are hardly visible, since they are weak calcined CoZSM5 exhibits Raman bands near 681, 530, and 485 cm^{-1} characteristic of the Co_3O_4 phase; the broad Raman band near 598 cm^{-1} is characteristic of surface amorphous cobalt oxide species [55]. Dispersed cobalt oxide rearranges to Co_3O_4 phase during reaction. Fresh PtCoZSM5 catalyst exhibits no Raman features of cobalt oxide species (Fig. 4B-a). During in situ treatment in He at 450 °C, a new Raman band near 598 cm^{-1} becomes evident (Fig. 4B-b); this band is characteristic of amorphous cobalt oxide species. Fig. 4C shows the TPR-Raman study of calcined CoZSM5. As the reduction temperature increases, Raman bands of Co_3O_4 decrease in intensity, and are almost absent by 500 °C. The weak regular pattern observed upon reduction is due to background signal, not related to the sample. The Raman band of dispersed Co oxides species appears less affected in this temperature range, but it significantly reduces its intensity by 600 °C. This result indicates that Co_3O_4 reduces at lower temperatures than surface amorphous cobalt oxide species. So, in CoZSM5, the presence of Co_3O_4, a good methane oxidation catalyst, deleteriously affects the N_2 selectivity. With the introduction of Pt, the Co^{2+} migrates to harder-to-reduce positions and Co_3O_4 is not formed.

3. Operando spectroscopy

In situ techniques provide a great approach to understanding catalysis. A further step is to study catalysts under genuine reaction conditions. This is the field of operando spectroscopy; the term operando comes from Latin and means working or operating [7,41–43,56,57]. This technology combines the characterization of the catalytic material with the simultaneous measurement of catalytic activity/selectivity (e.g. by mass spectrometry or gas chromatography, etc.). Operando studies provide molecular level information about the dynamic states

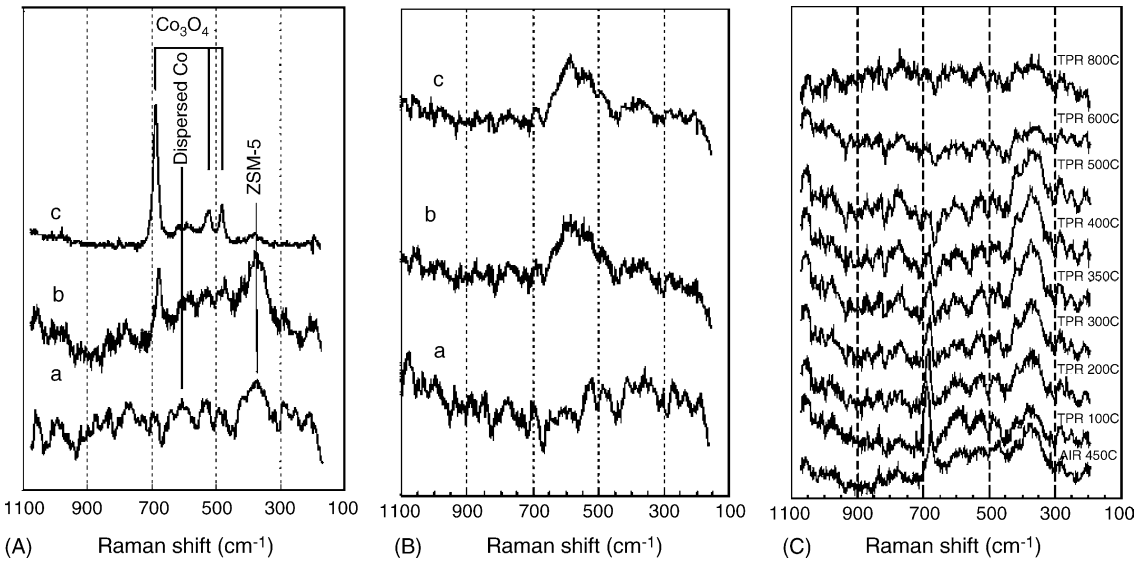

Fig. 4. (A) In situ Raman spectra of cation-exchanged ZSM5 recorded at 22 °C: (a) NaZSM5 calcined at 350 °C, (b) CoZSM5 calcined at 350 °C, and (c) used CoZSM5. (B) In situ Raman spectra of PtCoZSM5 calcined at 350 °C: (a) recorded at 22 °C and (b) recorded at 450 °C in He flow and (c) used under reaction conditions. (C) In situ Raman spectra of CoZSM5 calcined at 350 °C; reduced in situ with 1% H_2 in Ar. Reprinted from Ref. [54], with permission from Elsevier.

of catalytic active sites and about the surface reaction intermediates during catalytic reactions, where structure and activity are simultaneously being determined.

The operando methodology requires that the reaction take place in a reactor in which the spectroscopic characterization of the catalyst can be made. Many developments have been done towards this target. A few representative cases follow. Cheng et al. [58] designed an in situ cell with the catalyst sample as a wafer form on a rotor by 1980. Possibly, Hill and coworkers reported the earliest operando Raman study in 1991 [59]. Lunsford and coworkers [60] designed a Raman cell that minimizes void volume upstream the catalyst bed, which is in powder form and the gases flow through it. Volta and coworkers [47] developed a cell that rotates a lens distributing the laser spot around the sample, avoiding local heating at given spots. The operando Raman cell designed in our laboratory (Fig. 5) uses Raman microscope system in a fixed-bed microreactor with on-line gas chromatograph or mass spectrometer analysis of activity [61,62]. Activity and selectivity exhibit negligible differences between the operando reactor and a conventional fixed-bed microreactor [63]. This is a key difference between in situ cell and operando reactors. An operando reactor is one kind of in situ cell; as such, it requires nothing less than an in situ cell. But an operando reactor is also a catalytic reactor, not just a flow-through cell with on-line analysis. An operando reactor requires nothing less that the conventional reactor used for the reaction in study. Such combination of cell and reactor requirements defines the operando spectroscopic reactor. It is critical that the activity and kinetic data obtained in an operando reactor agree with those obtained in the corresponding conventional reactor [42,63]. The furnace is designed with a small opening that allows spectra acquisitions with a long distance objective and does not decrease the temperature locally. Weckhuysen use an operando reactor suitable for simultaneous Raman, UV–vis spectroscopy and synchrotron radiation [64]. The operando reactor designed by Mestl et al. uses a fiber optic Raman probe and a double bed configuration, which is intended to facilitate the equilibration of the bed under observation; on-line GC–MS provides simultaneous activity/selectivity data [65–67]. Stair group developed an in situ UV-Raman cell, where degradation problems of the sample may be more important due to their use of higher energy radiation; they used a fluidized bed with an in situ Raman cell [68].

Operando methodology facilitates structure–activity relationships at a molecular level since both, structure and activity are determined simultaneously. Some examples of operando Raman studies based in the authors work are presented with the aim of giving an overview of the capabilities of this powerful tool for the understanding of how catalysts work. The following examples try to illustrate the capabilities of operando Raman methodology in heterogeneous catalysts. These studies have been run at the Institute of Catalysis in Madrid, with the operando reactor shown in Fig. 5.

3.1. Mo–V/Al_2O_3 catalysts during propane oxidative dehydrogenation

The interactions between Mo and V on alumina were studied for the oxidative dehydrogenation of propane [63]. Fig. 6 shows the operando Raman-GC study of Mo–V/Al_2O_3 catalyst (6.0 wt.% V_2O_5, 9.2 wt.% MoO_3) at monolayer coverage during the oxidative dehydrogenation (ODH) of propane. At higher coverage, these catalysts exhibit efficient mixed Mo–V oxide phases [69]; however, such promotion was not observed near monolayer coverage [63]. The Raman bands of mixed Mo–V–O phases (762 cm^{-1}) [69] and V-distorted MoO_3 phases (965 and 783 cm^{-1}) [70] can be appreciated in the spectrum of fresh catalyst under dehydrated conditions. These structures change when propane reaction is observed. The Raman bands of Mo–V–O mixed phases are replaced by new Raman bands at

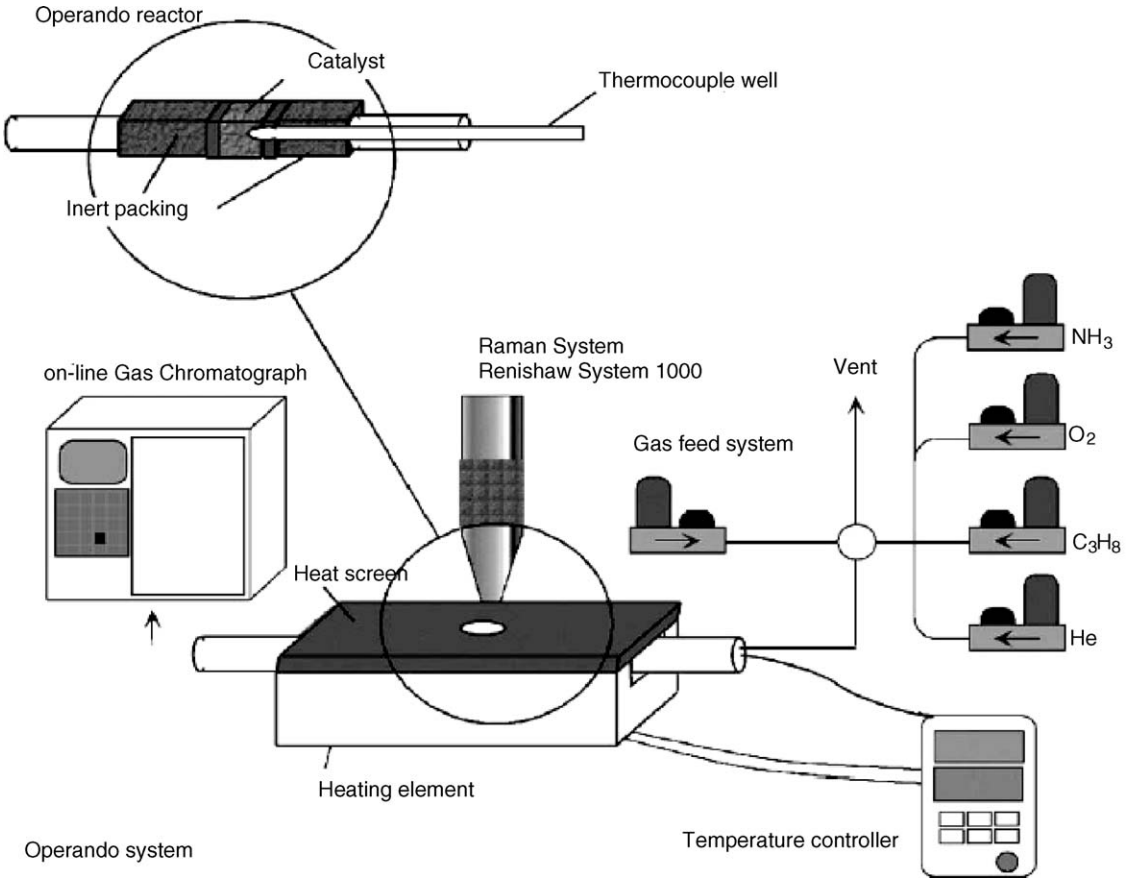

Fig. 5. Operando Raman-GC setup.

1025 and 1002 cm^{-1} characteristic of the V=O and Mo=O stretching modes of surface vanadia and molybdena species, respectively. Thus, at lower coverage, mixed Mo–V oxide phases on alumina are not stable and break spreading into the constituting oxides, which accounts for the lack of catalytic promotion. This underlines the relevance of in situ studies. The sample have been calcined at 450 °C in air, however, they break at spread at 300 °C in reaction. These oxides operate on a Mars–van-Krevelen mechanism, which involves lattice oxygen ions, this may account for a higher instability of the bulk Mo–V–O phase.

3.2. V/Al_2O_3 catalysts during propane oxidative dehydrogenation

The effect of O_2/C_3H_8 molar ratio in the performance and structure of supported vanadium oxide catalysts was studied during propane oxidative dehydrogenation [71]. Fig. 7 shows the Raman spectra, conversion, and product selectivities of VO_x/Al_2O_3 catalyst at different O_2/C_3H_8 molar ratio at 400 °C. During reaction with O_2/C_3H_8 = 10/1 feed, the catalyst shows Raman bands at 1026 and 1009 cm^{-1}, characteristic of the V=O mode. No appreciable effect is recorded on the structure

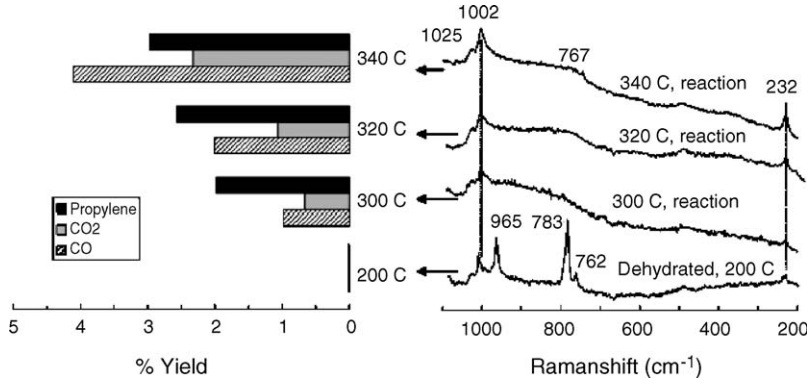

Fig. 6. Operando Raman-GC study of catalyst Mo–V/Al_2O_3 during propane ODH reaction (left panel). Conversion to the different products during Raman spectra acquisition (right panel), simultaneous Raman spectra. Reaction conditions: catalyst weight, 200 mg; total flow, 90 ml/min; reaction feed: O_2/C_3H_8/He = 1/12/8 M. Reprinted from Ref. [63], with permission from Elsevier.

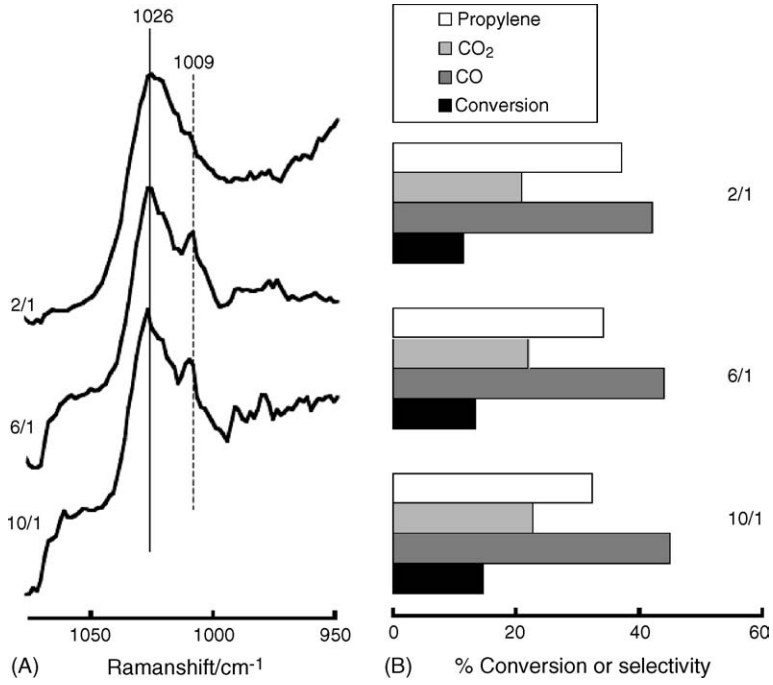

Fig. 7. Operando Raman spectra of VO_x/Al_2O_3 catalyst during propane ODH vs. O_2/C_3H_8 molar ratio at 400 °C reaction temperature (A) and conversion of propane and selectivity to CO, CO_2 and propylene (B). Reprinted from Ref. [71], with permission from Elsevier.

and activity as the O_2/C_3H_8 molar ratio decreases from 10/1 to 6/1 during reaction, at a constant propane partial pressure. This is normal under oxygen-rich reaction conditions. However, the spectrum with $O_2/C_3H_8 = 2/1$ exhibits only the Raman V=O mode at 1026 cm^{-1}. The catalytic performance shows negligible changes in the conversion and selectivity data (Fig. 7). Complementary UV–vis studies during reaction [66] show a moderate reduction of surface vanadium oxide on alumina during ODH reaction. This reduction is mainly due to the reduction of surface polymeric vanadium oxide species rather than the isolated ones [66]. Therefore, the Raman band at 1009 cm^{-1} should correspond to the V=O mode of isolated vanadium oxide species. It should be noted, that typically, the higher frequency appears to correspond to the polymeric vanadia species [85,86]. The results suggest that the activity and selectivity profiles of VO_x/Al_2O_3 catalyst are not affected by the loss of polymeric surface vanadia species. Thus, propane ODH does not require a special coordination of vanadia sites.

These VO_x/Al_2O_3 catalysts were also studied during propane oxidative dehydrogenation (ODH) and non-oxidative dehydrogenation (DH) at different temperatures [73]. Fig. 8A shows the operando Raman study during ODH and Fig. 8B during DH. The catalyst operates at steady state during propane ODH and the conversion increases with reaction temperature. The catalyst exhibits a Raman band at 1012 cm^{-1} and a broad band near 890 cm^{-1}, which correspond to the terminal V=O and V–O–V bonds vibration modes of surface-dispersed mono–oxo vanadium oxide species, respectively. These bands are not affected by the propane ODH reaction in the 573–673 K temperature range (Fig. 8A). So, the catalyst remains essentially oxidized during ODH reaction. This is in line with complementary reaction in situ UV–vis studies that show little reduction of alumina-supported catalysts under ODH conditions that evidence significant reduction of the vanadium sites under DH (oxygen-free) conditions [71]. Propane conversion is significantly lower in the absence of oxygen (Fig. 8B). The operando Raman-GC studies show no activity at low temperature (below 773 K) during DH reaction (Fig. 8B). A moderate decrease of the Raman modes of surface vanadium oxide species at 1012 and 890 cm^{-1} is observed as the temperature increases. This trend indicates a reduction of surface vanadium oxide species. This is consistent with reaction in situ UV–vis studies [72]. New features in the 1100–1700 cm^{-1} region are observed in the Raman spectra and a new broad band near 1600 cm^{-1} becomes evident at 673 K, this band is assigned to surface layers of sp^2 carbon species. The two bands near 1589 and 1327 cm^{-1} that appear as the temperature increases are indicative of sp^2 carbon in graphite-like materials [75–78]. Polyaromatics fluoresce and are not analyzable by visible Raman spectroscopy. UV-Raman can characterize them, and they possess several Raman modes between 1200 and 1700 cm^{-1} [79]. So, these studies show the formation of two types of carbonaceous deposits under propane DH conditions: one with a more aliphatic character at lower temperatures, and one with a graphitic character at higher temperatures. The concomitant formation of propene at the temperature at which graphite-like carbon deposits form underlines the relevance of propylene for coke formation. This is in line with Raman studies under propene feed [80]. On returning to ODH conditions, the carbon deposits are burnt right away and surface vanadium oxide species are restored. Similar results have been reported for supported chromia catalysts using operando UV–vis [74].

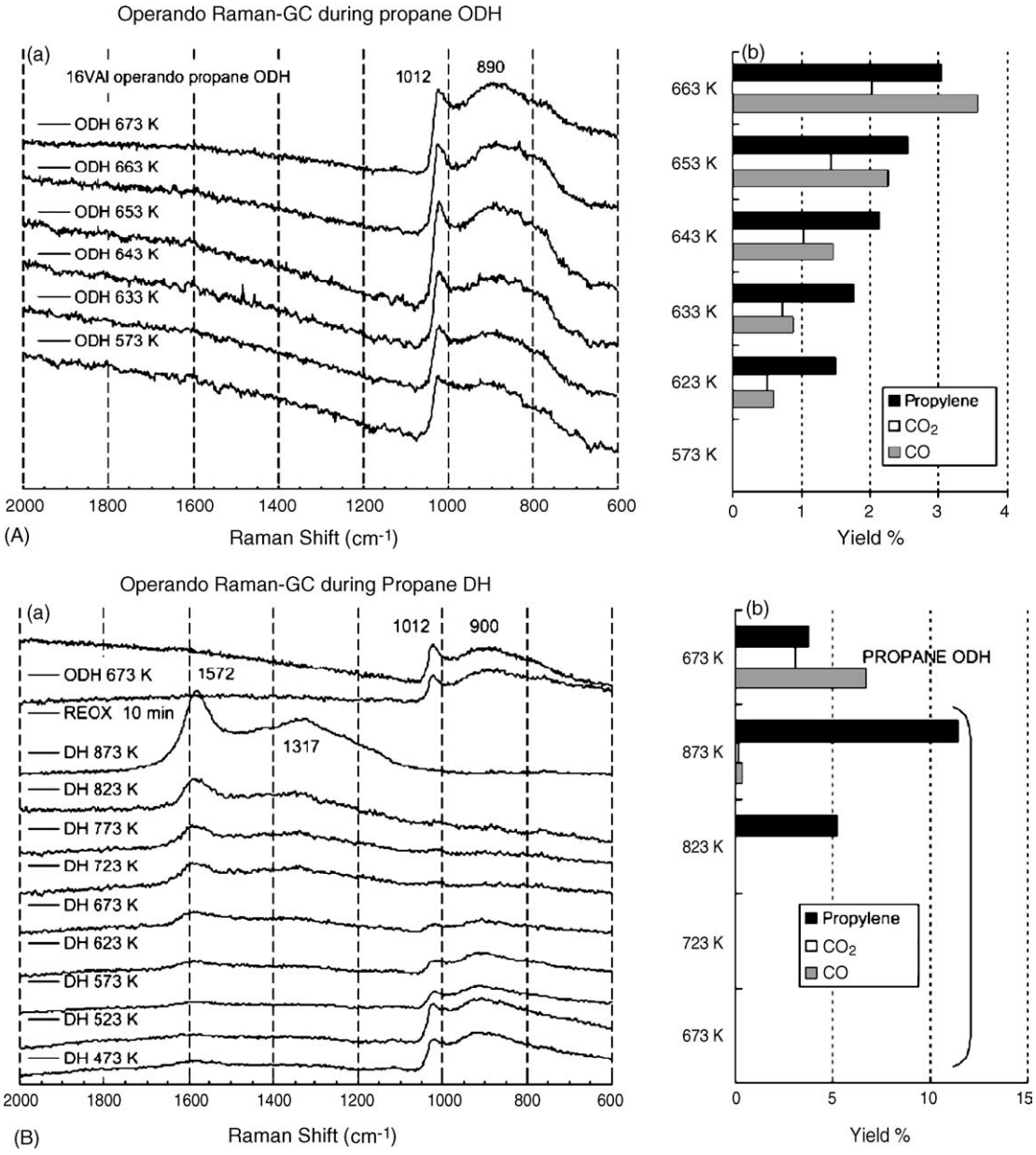

Fig. 8. (A) Operando Raman-GC study of VO_x/Al_2O_3 catalyst during propane ODH at different reaction temperatures (left) and activity data (right). (B) Operando Raman-GC study during propane DH reaction vs. reaction temperature. In situ reoxidized at 773 K after propane DH and operando Raman-GC during propane ODH at 673 K. Catalyst weight: 150 mg, total flow 67 ml min^{-1}, reaction feed propane/oxygen/helium:1/6/4 for ODH reaction and 1/0/6 for DH reaction. From Ref. [73] (reproduced by permission of the PCCP Owner Societies).

3.3. V–Sb/Al_2O_3 catalysts during propane ammoxidation to acrylonitrile

The determination of structure–activity relationships in supported oxides is rather convenient, since all the supported phase is typically exposed to the reactant, so that all the structural information of the active phase, corresponds to the phase exposed to the reactants. The determination of structure–activity relationships in bulk mixed-metal oxides presents a new variable. Raman spectroscopy is a bulk technique, and bulk mixed-metal oxides typically posses a small surface-to-volume ratio. Therefore, the signal from the bulk overwhelms the signal from the outermost layer. The outermost layer is the end of the tridimensional bulk pattern and is not like the bulk in addition, the nature of the outermost layer can be shaped by the reaction conditions. An approach to tackle this issue is to use nanoscaled mixed-metal oxides particles, with a very high surface-to-volume ratio. Because these may sinter during reaction, they should be stabilized. The interaction with a support where the mixed-metal oxides are deposited at total coverages ranging from one to few monolayers prevents their aggregation. Thus, mixed-metal oxides particles are restricted to few nanometers. We have used alumina-stabilized nanoscaled V–Sb–O catalyst for propane ammoxidation. Due to the high surface-to-volume ratio, it is possible to address the interactions between dispersed and bulk Sb and V sites during propane ammoxidation to

acrylonitrile [62,81]. The interaction between surface Sb (no Raman bands) and surface V oxide species (Raman bands at 1020 and 900 cm^{-1}) on alumina takes place under reducing or nonnet-oxidizing environments (e.g., ammoxidation reaction conditions) leading to the formation of $VSbO_4$ (broad Raman band at 840 cm^{-1}) [81,82] and segregated α-Sb_2O_4. The oxidation states in $VSbO_4$, are Sb(V) and V(III) [83,84]. The reduction of surface vanadium (V) species under ammoxidation conditions can be the driving force to build $VSbO_4$ during reaction.

The interaction between Sb and V appears partially reversed upon reoxidation, where V(III) species in $VSbO_4$ segregate as surface V(V) species [81]. This trend increases with the reoxidation temperature. Interestingly, a concomitant decrease of segregated α-Sb_2O_4 is evident, and the $VSbO_4$ phase does not appear significantly affected by these changes. Actually, $VSbO_4$ phase is rather stable under different environments (oxidizing and reducing) and accepts several stoichiometries close to $V_1Sb_1O_4$. Apparently, vanadia cations leave the $VSbO_4$ structure during reoxidation cycles and antimony enters it. A reverse trend is observed under ammoxidation reaction conditions. α-Sb_2O_4 is a mixed-valence oxide possessing Sb(III) and Sb(V) cations. Thus, it would make sense that such stability of the $SbVO_4$ phase must be due to a migration of the corresponding amount of Sb(V) cations from α-Sb_2O_4 into $VSbO_4$ to compensate the removal of V(III) cations. It is interesting to underline that surface vanadium species are pentavalent while bulk vanadium species in $VSbO_4$ are trivalent. This cycle appears to be the redox cycle for vanadium sites. The migration cycle of Sb (V) species would facilitate the redox cycle of vanadium species stabilizing the $VSbO_4$ lattice. This migration cycle of Sb and V species appears important for the propane ammoxidation reaction, and is consistent with the structural transformations observed in bulk vanadium antimonate catalysts.

4. Conclusions

The operando methodology combines both, structural and catalytic measurements, in a single experiment. Since the actual molecular structure of a catalyst depends on the specific environmental conditions, such combination is critical to assess structure–activity relationships at a molecular level reliably. Based on this premises, it is fundamental that both information are reliable. The characterization must provide information relevant to the catalytic process, i.e. about the phases directly interacting with the reactants. The activity data must be genuine catalytic data; therefore, the design of the Raman cell and the reaction conditions are critical to prevent any mass or heat transfer limitation or the contribution of non-catalytic reactions, e.g. gas-phase reaction.

Acknowledgements

This research has been funded by MAT-2002-C02-0400 by the Ministry of Education and Science, Spain and by ESF COST Action D15/0021/01. MOGP acknowledges the Ministry of Education and Science for a ‘‘Juan de la Cierva’’ postdoctoral position at the University of Málaga, Spain.

References

[1] E.V. Hoefs, J.R. Monnier, G.W. Keulks, J. Catal. 57 (1979) 331.
[2] G.A. Somorjai, G. Rupprechter, J. Phys. Chem. B 103 (1999) 1623.
[3] G.A. Somorjai, Chem. Rev. 96 (1996) 1223.
[4] H.E. Shih, F. Jona, P.M. Marcus, Phys. Rev. Lett. 46 (1981) 731.
[5] Y. Gauthier, R. Baudoing-Savois, K. Heinz, H. Landskron, Surf. Sci. 251 (1991) 493.
[6] H. Topsøe, Stud. Surf. Sci. Catal. 130A (2000) 21.
[7] B.M. Weckhuysen, Chem. Commun. (2002) 97.
[8] M.A. Bañares, In situ raman spectroscopy, in: B.M. Weckhuysen (Ed.), In Situ Characterization of Catalysts, American Scientific Publishers, 2004.
[9] I.E. Wachs, in: I.R. Lewis, H.G.M. Edwards (Eds.), Handbook of Spectroscopy, Marcel Dekker, New York, 2001.
[10] J.R. Bartlett, R.P. Cooney, in: R.J.H. Clark, R.E. Hester (Eds.), Spectroscopy of Inorganic-based Materials, Advances in Spectroscopy, vol. 14, Wiley, Chichester, 1987, p. 187.
[11] M. Mehicic, J.G. Grasselli, in: J.G. Grasselli, B.J. Bulkin (Eds.), Analytical Raman Spectroscopy, Wiley, Chichester, 1991, p. 325.
[12] L. Dixit, D.L. Gerrard, H.J. Bowley, Appl. Spectrosc. Rev. 22 (1986) 189.
[13] I.E. Wachs, F.D. Hardcastle, Catalysis, vol. 10, The Royal Society of Chemistry, Cambridge, 1993, p. 102.
[14] E. Garbowski, G. Coudurier, in: B. Imelik, J.C. Vedrine (Eds.), Catalyst Characterization. Physical Techniques for Solid Materials, Plenum Press, New York, 1994, p. 45.
[15] G. Mestl, H. Knözinger, in: G. Ertl, H. Knözinger, J. Weitkamp (Eds.), Handbook of Heterogeneous Catalysis, vol. 2, Wiley/VCH, Weinheim, 1997, p. 539.
[16] J.M. Stencel, Raman Spectroscopy for Catalysis, Van Nostrand, Reinhold, New York, 1990.
[17] R.P. Cooney, G. Curthoys, T.T. Nguyen, Adv. Catal. 24 (1975) 293.
[18] T.A. Egerton, A.H. Hardin, Catal. Rev. Sci. Eng. 11 (1975) 1.
[19] W.N. Delgass, G.L. Haller, R. Kellerman, J.H. Lunsford, Spectroscopy in Heterogeneous Catalysis, Academic Press, New York, 1979, pp. 55–58.
[20] B.A. Morrow, in: A.T. Bell, M.L. Hair (Eds.), Vibrational Spectroscopy of Adsorbed Species, ACS Symposium Series, vol. 137, ACS, Washington, DC, 1981, p. 119.
[21] T. Takenaka, Adv. Colloid. Interface Sci. 11 (1979) 291.
[22] T.T. Nguyen, J. Singapore Natl. Acad. Sci. 10–12 (1983) 84.
[23] N. Sheppard, J. Erkelens, Appl. Spectrosc. 38 (1984) 471.
[24] M.A. Chesters, N. Sheppard, Chem. Br. 17 (1981) 521.
[25] K. Segawa, I.E. Wachs, in: I.E. Wachs (Ed.), Characterization of Catalytic Materials, Butterworth/Heinemann, Boston, 1992.
[26] I.E. Wachs, F.D. Hardcastle, S.S. Chan, Spectroscopy 1 (1986) 30.
[27] H. Knözinger, in: H.H. Brongersma, R.A. van Santen (Eds.), Characterization of Heterogeneous Catalysis studied by Particle Beams, Plenum Press, New York, 1991, p. 167.
[28] G. Mestl, T.K.K. Srinivasan, Catal. Rev. Sci. Eng. 40 (1998) 451.
[29] I.E. Wachs, Top. Catal. 8 (1999) 57.
[30] M.A. Bañares, Raman Spectroscopy, in: B.M. Weckhuysen (Ed.), In Situ Characterization of Catalytic Materials, American Scientific Publishers, 2004.
[31] S.I. Woo, C.G. Hill, J. Mol. Catal. 29 (1985) 231.
[32] P.R. Carey, J. Raman Spectrosc. 29 (1998) 7.
[33] M.A. Bañares, I.E. Wachs, J. Raman Spectrosc. 33 (2002) 359.
[34] J.M. Thomas, Ang. Chem. Int. Ed. 38 (1999) 3588.
[35] P. Stair, Curr. Opin. Solid State Mater. Sci. 5 (2001) 365.
[36] S. Kuba, H. Knözinger, J. Raman Spectrosc. 33 (2002) 325.
[37] G. Mestl, J. Mol. Catal. A 158 (2000) 45.
[38] H. Knözinger, G. Mestl, Top. Catal. 45 (1999) 8.
[39] H. Knözinger, Catal. Today 32 (1996) 71.
[40] I.E. Wachs, Top. Catal. 57 (1999) 8.
[41] I.E. Wachs, Surf. Sci. 1 (2003) 544.
[42] M.A. Bañares, Catal. Today 100 (2005) 71.

[43] M.A. Bañares, G. Mestl, in preparation.
[44] S. Damyanova, L.M. Gomez, M.A. Bañares, J.L.G. Fierro, Chem. Mater. 12 (2000) 501.
[45] M.A. Carreón, V.V. Guliants, Micropor. Mesopor. Mater. 55 (2002) 304.
[46] M.A. Carreón, V.V. Guliants, M.O. Guerrero-Pérez, M.A. Bañares, Micropor. Mesopor. Mater. 71 (2004) 57.
[47] F. Ben Abdelouahab, R. Olier, N. Guilhaume, F. Lefebvre, J.C. Volta, J. Catal. 134 (1992) 151.
[48] F. Tuinstra, J.L. Koenig, J. Chem. Phys. 33 (1970) 1126.
[49] M.A. Bañares, J.H. Cardoso, F. Agulló-Rueda, J.M. Correa-Bueno, J.L.G. Fierro, Catal. Lett. 64 (2000) 191.
[50] N. Das, H. Eckert, H. Hu, I.E. Wachs, J.F. Walzer, F.J. Feher, J. Phys. Chem. 97 (1993) 8240.
[51] S. Xie, E. Iglesia, A.T. Bell, Langmuir 16 (18) (2000) 7162.
[52] M.E. Harlin, V.N. Niemi, A.O.I. Krause, J. Catal. 195 (2000) 67.
[53] J. Kanervo, M.E. Harlin, A.O.I. Krause, M.A. Bañares, Catal. Today 78 (2003) 171.
[54] A. Boix, E.E. Miró, E.A. Lombardo, M.A. Bañares, R. Mariscal, J.L.G. Fierro, J. Catal. 217 (2003) 186.
[55] M.A. Vuurman, D.J. Stufkens, A. Oskam, G. Deo, I.E. Wachs, Chem. Soc., Faraday Trans. 92 (1996) 3259.
[56] M.A. Bañares, M.O. Guerrero-Pérez, J.L.G. Fierro, G.G. Cortez, J. Mater. Chem. 12 (2002) 3337.
[57] I.E. Wachs, Catal. Commun. 4 (2003) 567.
[58] C.S. Cheng, J.D. Ludowise, G.L. Schrader, Appl. Spectrosc. 146 (1980) 34.
[59] J.H. Wilson, C.G. Hill, J.A. Dumesic, J. Mol. Catal. 61 (1990) 333.
[60] G. Mestl, M.P. Rosynek, J.H. Lunsford, J. Phys. Chem. B 101 (1997) 9321.
[61] M.A. Bañares, M.V. Martínez-Huerta, X. Gao, J.L.G. Fierro, I.E. Wachs, Metaloxide Catalysts: Active Sites, Intermediates and Reaction Mechanisms 220 ACS Symposium, Washington, USA, 2000.
[62] M.O. Guerrero-Pérez, M.A. Bañares, Catal. Today. 96 (2004) 265.
[63] M.A. Bañares, S.J. Khatib, Catal. Today 96 (2004) 251.
[64] B.M. Weckhuysen, Phys. Chem. Chem. Phys. 5 (2003) 4351.
[65] G. Mestl, C. Linsmeier, R. Gottschall, M. Dieterle, J. Find, D. Herein, J. Jäger, Y. Uchida, R. Schlögl, J. Mol. Catal. A: Chem. 270 (2000) 455.
[66] M. Dieterle, G. Mestl, J. Jäger, Y. Uchide, R. Schlögl, J. Mol. Catal. A: Chem. 174 (2001) 169.
[67] O. Ovsitser, A. Blume, Y. Uchida, G. Mestl, R. Schögl, J. Mol. Catal. A: Chem (2002).
[68] Y.T. Chua, P.C. Stair, J. Catal. 196 (2000) 66.
[69] H. Dai, A.T. Bell, E. Iglesia, J. Catal. 221 (2004) 491.
[70] Wachs I.E. Personal communication
[71] G. García Cortez, M.A. Bañares, J. Catal. 209 (2002) 197.
[72] X. Gao, M.A. Bañares, I.E. Wachs, J. Catal. 188 (2) (1999) 325.
[73] G. Mul, M. A: Bañares, G.G. Cortez, B. Van der Linden, S.J. Khatib, J.A. Moulijn, Phys. Chem. Chem. Phys. 5 (2003) 4378.
[74] T.A. Nijhuis, S.J. Tinnemans, T. Visser, B.M. Weckhuysen, Phys. Chem. Chem. Phys. 5 (2003) 4361.
[75] R.J. Nemanich, S.A. Solin, Phys. Rev. B 20 (1979) 392.
[76] N.B. Colthup, L.H. Daly, S.E. Weberley, Infrared and Raman Spectroscopy, 3rd ed., Academic Press, New York, 1990.
[77] A. Cuesta, P. Dhamelincourt, J. Laureys, A. Martínez-Alonso, J.M.D. Tascón, Carbon 32 (1994) 1523.
[78] G. Katagiri, H. Ishida, A. Ishitani, Carbon 2 (1988) 565.
[79] Y.T. Chua, P.C. Stair, J. Catal. 213 (2003) 39.
[80] M.A. Bañares, G. Mul, S. Khatib, J.A. Moulijn, in preparation.
[81] M.O. Guerrero-Pérez, M.A. Bañares, Chem. Commun. (2002) 1292.
[82] G. Xiong, V.S. Sullivan, P.C. Stair, G.W. Zajac, S.S. Trail, J.A. Kaduk, J.T. Golab, J.F. Brazdil, J. Catal. 230 (2005) 326.
[83] T. Birchall, A.W. Sleight, Inorg. Chem. 15 (1976) 868.
[84] F.J. Berry, M.E. Brett, Inorg. Chim. Acta 7 (1983) L205.
[85] Z. Wu, H.S. Kim, P.C. Stair, S. Rugmini, S.D. Jackson, J. Phys. Chem. B 109 (2005) 2793.
[86] M.A. Vuurman, I.E. Wachs, J. Phys. Chem. 96 (1992) 5008.